Eng. Cov & Innov. An Int. J. Volume 01, Issue 01, January – April, 2026

Universal Research Forum
Engineering Convergence and Innovation (ECI) An International Journal
www.universalresearchforum.com

Mathematical and Finite Element Modeling of Equal Channel Angular Extrusion: A Short Review

Gajanan M Naik[1]*, Sadashiv Bellubbi[2], Ramesh S[3]

[1]Department of Mechanical Engineering, RV Institute of Technology and Management Bengaluru, Karnataka-560076, India
[2]Department of Mechanical Engineering, Jain College of Engineering and Research, Udyambag-590008, Belagavi Karnataka, India.
[3]School of Computer science and engineering, RV University, Mysore Rd, RV Vidyaniketan Post Bengaluru 560058, Karnataka, India.
*Email.:gajamnaik@gmail.com & Mob: +91 7760006193

Published Date: 21 October 2025.

ABSTRACT

Literature review on mathematical and FE modelling of developed strain distribution during ECAE process is reviewed and analyzed. From the last few decades, a variety of models have been developed and discussed at different aspects of ECAP. In hypothesis, the developed strain during ECAP depends on the geometry of the ECAP die, which is die channel angle (ϕ) and corner angle (ψ). This short review critically reviews the mathematical models of ECAE process and impact of ECAP die angles on deformation homogeneity through finite element methods.

Keywords - *Channel angle, Corner angle, ECAP, FEM, Hall-Petch.,*

1. INTRODUCTION to ECAP

Equal channel angular extrusion process created by Segal [1], is the most utilized severe plastic deformation method for material grain refining, resulted in a boost of mechanical and physical properties to achieve superplastic behavior [2-4]. During ECAP material is pushed through two intersecting equal channel of having die angles which accumulates very large plastic strain without altering the materials' geometric cross-section. There exist five major processing routes like Route A: sample processes without rotation, Route BA:, Route Bc: Route C: [5] between passes, Route R: [6-10]. Until now numerous scholars contributed to investigating the importance of processing routes, which gives rise to route Bc and Route R are efficient processing routes to alter the shear band inclinations of the metal crystal structure and to create varies microstructure and texture [11]. Moreover, mathematical modelling for this process is the foremost step to determine plastic strain distribution in the processing material which is based on the geometric of the ECAP die. This paper reviews the mathematical and FEM modelling of ECAP for better understanding and to relate the actual process.

2. MATHEMATICAL MODEL

The Hall and Petch, have been conducted experimental and theoretical studies to illustrate the linear relationship between yield stress and the grain size (d) given in equation (1) [12].

$$\sigma_y = \sigma_0 + \frac{k_y}{\sqrt{d}} \qquad (1)$$

2.1 ESTIMATION OF THE STRAIN AND CRITICAL GRAIN SIZE IN ECAP PROCESSING.

Yoshinori et al.[13] have reported estimation of equivalent train rate by considering the geometry. The geometries of ECAP is presented in Fig 1. Where two channels intersect at channel angle ϕ and corner angle Ψ. During this study, author has considered circumstances, where corner angle Ψ lies between 0 to (Π-ϕ). Channel wall friction of die can be avoided by using a proper lubricant. Therefore frictional effects were neglected. Therefore, the shear strain can be given by

$$\gamma = 2\cot\left(\frac{\phi+\Psi}{2}\right) + \Psi \operatorname{cosec}\left(\frac{\phi+\Psi}{2}\right) \quad (2)$$

And equivalent strain for N number of passes;

$$\varepsilon_{eq} = \frac{N}{\sqrt{3}}\left(2\cot\left(\frac{\phi+\Psi}{2}\right) + \Psi \operatorname{cosec}\left(\frac{\phi+\Psi}{2}\right)\right) \quad (3)$$

γ is shear strain, ε_{eq} equivalent strain, N number of ECAP passes, 1,2,…n

When, N is equal to one pass, a) Ψ= 0, b) Ψ = (Π-ϕ), the equation (2) becomes

$$\varepsilon_{eq} = \frac{1}{\sqrt{3}}\left(2\cot\left(\frac{\phi+\Psi}{2}\right) + \Psi\right) \quad (4)$$

$$\varepsilon_{eq} = \frac{1}{\sqrt{3}}\Psi \quad (5)$$

Thus, the equivalent strain rate of ECAP of any number of passes can be estimated through equation (3) [13, 10]. Flávia et al. [14] have discussed the importance of critical diameter of the grains. From the study, it was observed that the grain size of material less than the critical diameter of grain which gives the homogeneous or uniform grain (d<dc1). The critical grain size of the specific materials can be calculated through a theoretical model given in equation (6).

$$d_{c1} = q.\delta.\frac{1-q^2}{2\,q}\left(1 - 2\,\frac{\tau_m^*}{K_m}\sqrt{\frac{\delta(1-q^2)}{2q}}\right) \quad (6)$$

When q =0.2, equation (6) yields the critical grain size $dc_1 \approx 22\delta = 022$ nm which matches to the volume fraction of boundaries c ≈ 0.12 [14].

2.2 Upper-bound Theorem

Medeirosa et al. [15] have discussed, an analytical model to estimate the extrusion pressure to perform the equal channel angular pressing of was considered for rectangular section, using upper bound theorem proposed by Pérez & Luri, considering all geometry parameters of the ECAP die, displayed in Figure 1. The theoretical predictions of pressing pressure for rectangular specimen are given in equation (7) and (8). This is based on the inner and outer radii of the channel [16-18].

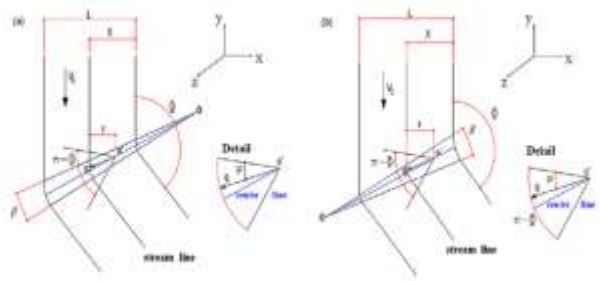

Fig 1. ECAP die geometries considered to calculate extrusion pressure (a) $R_{inner} < R_{outer}$ and (b) $R_{inner} > R_{outer}$ [14,16,18].

$$P = LWk\left\{\frac{(\Pi-\phi)}{Sin\,((\phi+\beta)/2)} + f\left[\frac{2H}{L} + (\Pi - \phi)\left(\frac{R_{inner}+R_{outer}}{L}\right)\left(1 - \frac{1}{\sin((\phi+\beta)/2)}\right) + \frac{2H}{W}\right]\right\}$$

For $R_{inner} < R_{outer}$ (7)

$$P = LWk\left\{\frac{(\Pi-\phi)}{Sin\,((\phi-\beta)/2)} + f\left[\frac{2H}{L} + (\Pi - \phi)\left(\frac{R_{inner}+R_{outer}}{L}\right)\left(1 - \frac{1}{\sin((\phi-\beta)/2)}\right) + \frac{2H}{W}\right]\right\}$$

For $R_{inner} > R_{outer}$ (8)

$$\beta = 2\arctan\left\{\frac{(R_{inner}-R_{outer})\tan(\phi/2)}{L+(R_{inner}-R_{outer})+L\,tan^2(\phi/2)}\right\} \quad \text{for } R_{inner} < R_{outer} \quad (9)$$

$$\beta = 2\arctan\left\{\frac{(R_{outer}-R_{inner})\tan(\phi/2)}{L+(R_{inner}-R_{outer})+L\,tan^2(\phi/2)}\right\} \quad \text{for } R_{inner} > R_{outer} \quad (10)$$

From equation (11) and (12) indicates the deformation time during which material undergoes ECAP deformation.

$$t_D = \frac{L}{V_o}\left\{2\,cotan\left(\frac{\phi+\beta}{2}\right) + \frac{(\pi-\phi)}{L}\left(1 - cotan\left(\frac{\phi+\beta}{2}\right)\tan\left(\frac{\phi}{2}\right)\right)\left[R_{inner} + L\left(1 - cotan\left(\frac{\phi+\beta}{2}\right)\tan\left(\frac{\phi}{2}\right)\right)\right]\right\}$$

for $R_{inner} < R_{outer}$ (11)

$$t_D = \frac{L}{V_o}\left\{2\,cotan\left(\frac{\phi-\beta}{2}\right) + \frac{(\pi-\phi)}{L}\left(1 - cotan\left(\frac{\phi-\beta}{2}\right)\tan\left(\frac{\phi}{2}\right)\right)\left[R_{inner} + L\left(1 - cotan\left(\frac{\phi-\beta}{2}\right)\tan\left(\frac{\phi}{2}\right)\right)\right]\right\} \quad \text{for } R_{inner} > R_{outer} \quad (12)$$

Rodrigo Luri et al. [19] have applied upper bound theorem to determine the force required to perform the ECAP process by considering circular cross-section, the equation (13) and (14) gives the predicated load based on ECAP die geometry. Also predicted equation for exit length (Ls) of the material has given in equation (15) and (16).

$$F = \frac{\sigma_o}{\sqrt{3}} \pi \left(D/2\right)^2 \frac{(\pi-\phi)}{\sin\left(\frac{\phi}{2}+\frac{\psi}{2}\right)} + m \frac{\sigma_o}{\sqrt{3}} \pi D \left[\left(L_E + D\cot\left(\frac{\phi}{2}+\frac{\psi}{2}\right) + L_s\right) + \frac{(\pi-\phi)}{\sin\left(\frac{\phi}{2}+\frac{\psi}{2}\right)}\left(\frac{R_{int}+R_{ext}}{2}\right)\right]$$

if $R_{inner} < R_{outer}$ (13)

$$F = \frac{\sigma_o}{\sqrt{3}} \pi \left(D/2\right)^2 \frac{(\pi-\phi)}{\sin\left(\frac{\phi}{2}-\frac{\psi}{2}\right)} + m \frac{\sigma_o}{\sqrt{3}} \pi D \left[\left(L_E + D\cot\left(\frac{\phi}{2}-\frac{\psi}{2}\right) + L_s\right) + \frac{(\pi-\phi)}{\sin\left(\frac{\phi}{2}-\frac{\psi}{2}\right)}\left(\frac{R_{int}+R_{ext}}{2}\right)\right]$$

if $R_{inner} > R_{outer}$ (14)

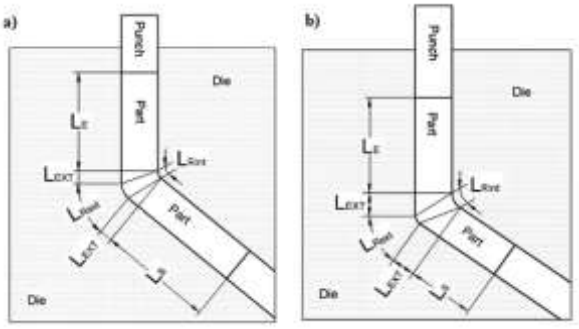

Fig 2. Surface contact parameters a) ECAP dies with $R_{int} < R_{ext}$, b) ECAP dies with $R_{int} > R_{ext}$ [8]

$$L_s = L_{init} - D\cot\left(\frac{\phi}{2}+\frac{\psi}{2}\right) - \frac{(\pi-\phi)}{\sin\left(\frac{\phi}{2}+\frac{\psi}{2}\right)}\left(\frac{R_{int}+R_{ext}}{2}\right) - L_E \quad \text{if } R_{inner} < R_{outer} \quad (15)$$

$$L_s = L_{init} - D\cot\left(\frac{\phi}{2}-\frac{\psi}{2}\right) - \frac{(\pi-\phi)}{\sin\left(\frac{\phi}{2}-\frac{\psi}{2}\right)}\left(\frac{R_{int}+R_{ext}}{2}\right) - L_E \quad \text{if } R_{inner} > R_{outer} \quad (16)$$

Where D is the diameter of the channel, m is friction coefficient, L_E length of the materials at the entrance channel, L_{int} initial length of the specimen shown in figure 2. Similarly, Rejaeian and Aghaie-Khafri. [20] Have employed the upper bound model to estimate an approximate force (eq.17) required to press the square billet of size 5mmx5mmx12mm through ECAP.

$$F = \frac{\sigma_o}{\sqrt{3}} DW\frac{(\pi-\phi)}{\sin\left(\frac{\phi}{2}+\frac{\psi}{2}\right)} + m \frac{\sigma_o}{\sqrt{3}}\left[w\left(2L_{initial} + (\pi-\phi)(R_{int}+R_{ext})\left(1-\frac{1}{\sin\left(\frac{\phi}{2}+\frac{\psi}{2}\right)}\right)\right) + D(2L_{initial})\right] \quad (17)$$

In Equation (5) m is a friction factor, 0<m<1, and factor L_{init} is the length of the sample. W and D are the width of the work-piece in the perpendicular and parallel directions to the symmetry plane, correspondingly [21].

2.3 DISLOCATION DENSITY-BASED STRAIN-HARDENING MODEL

Vaseghi [22] have established the Dislocation density-based strain-hardening model to explain the deformation behaviour of aluminum subjected to ECAP. Further, this methodology collective with the dynamic strain ageing. Consequently, this enables the simultaneous measurement of the strain hardening and microstructure evolution. Also, the enhancement of work hardening rate is because of an improvement in dislocation multiplication rate of dislocation locking by precipitates and the resulting creation of fresh mobile dislocations is the dominating processes controlling the high rate of strain hardening. The change of total dislocation density with strain is

$$\frac{d\rho}{d\epsilon} = (U\text{-}A) + Q_\rho \quad (18)$$

$$\rho = f\rho_w + (1\text{-}f)\rho_c \quad (19)$$

Where, U, represents the dislocations; Q, quantifies the likelihood for mobile dislocation generation; A, represents the immobilization rate of mobile dislocations at the precipitate-matrix interface.

2.4 FEM

Numerous scholars investigated result of die factors on the homogeneity of deformation, plastic-stress & strain using FE analysis. Djavanroodi [23] had studied the influence of the die angle and c.o.f on the deformation performance of Al alloy during the process of ECAP using FE technique. The results were conducted considering the channel angle 60.0º, 75.0º, 110.0º, 120.0º and constant ψ 25.0º and c.o.f of 0.0010 & 0.30, respectively. The results indicated that the amount of strain, rises by lessening in the ϕ of the die in ECAP and increase the c.o.f. Djavanroodi et al. [24] modeled four die channel angles combinations like ϕ = 60.0º, 90.0º, 105.0º and 120.0º and ψ = 0.0º, 15.0º and pass numbers till 8P have been modeled by the route. Rejaeian et al. [25] introduce the analytical models and finite element method to determine strain imposed to a sample which was deformed using ECAP. Also, inhomogeneity of strain in terms of the coefficient of deviation (CV) for an AA6101 aluminum alloy processed via ECAP was determined. Models of dies with intersecting angles of 90º, 105º and 120º were simulated using FEM. It has been established that inhomogeneity of strain becomes greater as the intersection angle between two channels diminishes. Patil et al. [26] From the simulation, the influence of channel angle (ϕ) on peak pressure was observed primarily. From the research as well, the information is disclosed that to obtain the desired strain channel angle (ϕ) and corner angle (ψ) are most crucial die parameters. Along with this, Park & Suh [27]

researcher models the effect heavily reported in the literature with the aid of finite element analysis (FEA). Ding et al. [28]. Furthermore, from this research, it was concluded that the use of lower ECAP processing temperature provides the fine grain structure and enhanced tensile strength.

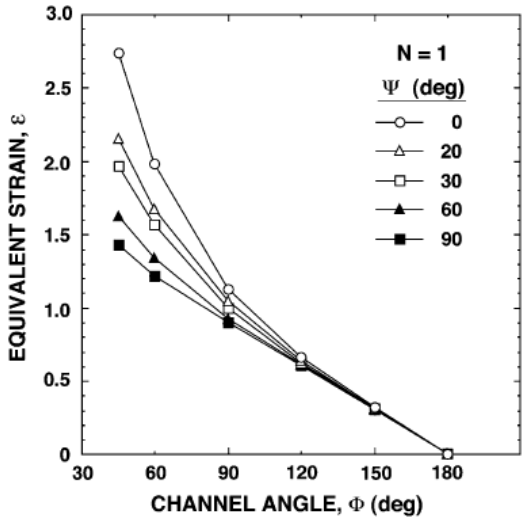

Fig 3. Equivalent strain versus channel angle for different arc of curvature [33]

3. CONCLUSION

This short-review is divided into two sections. In the first section, various characteristic models to describe the deformation in the course of ECAP were reviewed. In the second section, discussed the FEM simulation gave about the effect of die angles and c.o.f on deformation homogeneity and discussed the latest literature regarding the experimental study on the influence of die parameters on several response parameters including microstructure, mechanical and corrosion properties. As part of a brief review after conclusion is drawn.

- An upper-bound theory has been applied for ECAP, based on the analysis it was noticed that the ECAP parameters influencing the ECAP pressure and load can be ordered as (1) friction factor, (2) intersection angle of die channels, (3) outer and (4) inner die corners fillet radii and finally, (5) plunger speed.
- The angle of the die channel (ϕ) contributes extensively to billet deformation. Strain inhomogeneity is observed to increase when the angle of the die between channels is smaller.
- Increase in ECAP passes result in fine grain microstructure, homogeneous distribution of secondary phase, improved mechanical properties and corrosion resistance.

REFERENCE

[1] Djavanroodi, F., Omranpour, B., Ebrahimi, M., & Sedighi, M. (2012). Designing of ECAP parameters based on strain distribution uniformity. Progress in natural science: Materials international, 22(5), 452-460.

[2] Abd El Aal, M. I. (2017). 3D FEM simulations and experimental validation of plastic deformation of pure aluminum deformed by ECAP and combination of ECAP and direct extrusion. Transactions of Nonferrous Metals Society of China, 27(6), 1338-1352.

[3] Avvari, M., & Narendranath, S. (2014). Influence of Route-R on wrought magnesium AZ61 alloy mechanical properties through equal channel angular pressing. Journal of Magnesium and Alloys, 2(2), 159-164.

[4] Avvari, M., & Narendranath, S. (2014). Influence of Route-R on wrought magnesium AZ61 alloy mechanical properties through equal channel angular pressing. Journal of Magnesium and Alloys, 2(2), 159-164.

[5] Gajanan, M. N., Narendranath, S., & Kumar, S. S. (2019, August). Effect of grain refinement on mechanical and corrosion behavior of AZ91 magnesium alloy processed by ECAE. In IOP Conference Series: Materials Science and Engineering (Vol. 591, No. 1, p. 012015). IOP Publishing.

[6] Naik, G. M., Narendranath, S., Satheesh Kumar, S. S., & Sahu, S. (2019). Effect of annealing and aging treatment on pitting corrosion resistance of fine-grained Mg-8% Al-0.5% Zn alloy. JOM, 71(12), 4758-4768.

[7] Naik, G. M., Sannayellappa, N., & Satheesh Kumar, S. S. (2019). Corrosion of ECAPed Magnesium alloys and its background: A review. Journal of Metals, Materials and Minerals, 29(2), 1-20.

[8] Naik, G. M., Gote, G. D., Narendranath, S., & Kumar, S. S. (2018). The impact of homogenization treatment on microstructure microhardness and corrosion behavior of wrought AZ80 magnesium alloys in 3.5 wt% NaCl solution. Materials Research Express, 5(8), 086513.

[9] Naik, G. M., Gote, G. D., & Narendranath, S. (2018). Microstructural and hardness evolution of AZ80 alloy after ECAP and post-ECAP processes. Materials Today: Proceedings, 5(9), 17763-17768.

[10] Tański, T., Snopiński, P., Pakieła, W., Borek, W., Prusik, K., & Rusz, S. (2016). Structure and properties of AlMg alloy after combination of ECAP and post-ECAP ageing. Archives of civil and mechanical engineering, 16(3), 325-334.

[11] Naik, G. M., Gote, G. D., & Kumar, S. S. (2018). Effect of grain refinement on the performance of AZ80 Mg alloys during wear and corrosion. Advances in Materials Research, 7(2), 105.

[12] Gajanan, M. N., Narendranath, S., & Kumar, S. S. (2019, March). Influence of ECAP processing routes on microstructure mechanical properties and corrosion behavior of AZ80 Mg alloy. In AIP Conference Proceedings (Vol. 2082, No. 1, p. 030016). AIP Publishing LLC.

[13] Iwahashi, Y., Horita, Z., Nemoto, M., Wang, J., & Langdon, T. G. (1996). Principle of equal-channel angular pressing for the processing of ultra-fine grained materials. Scripta materialia, 35(2).

[14] Poggiali, F. S. J., Silva, C. L. P., Pereira, P. H. R., Figueiredo, R. B., & Cetlin, P. R. (2014). Determination of mechanical anisotropy of magnesium processed by ECAP. Journal of Materials Research and Technology, 3(4), 331-337.

[15] Medeiros, N., Moreira, L. P., Bressan, J. D., Lins, J. F. C., & Gouvêa, J. P. (2010). Upper-bound sensitivity analysis of the ECAE process. Materials Science and Engineering: A, 527(12), 2831-2844.

[16] Silva, F. R. F., Medeiros, N., Moreira, L. P., Lins, J. F. C., & Gouvêa, J. P. (2012). Upper-bound and finite-element analyses of non-isothermal ECAP. Materials Science and Engineering: A, 546, 180-188.

[17] Medeiros, N. D., Moreira, L. P., Bressan, J. D., Lins, J. F. C., & Gouvêa, J. P. D. (2010). Sensitivity analysis of the ECAE process via 2k experiments design. Matéria (Rio de Janeiro), 15, 208-217.

[18] Medeiros, N., Moreira, L. P., Bressan, J. D., Lins, J. F. C., & Gouvêa, J. P. (2010). Upper-bound sensitivity analysis of the ECAE process. Materials Science and Engineering: A, 527(12), 2831-2844.

[19] Luri, R., & Luis Pérez, C. J. (2012). Modeling of the processing force for performing ECAP of circular cross-section materials by the UBM. The International Journal of Advanced Manufacturing Technology, 58(9), 969-983.

[20] Aghaie-khafri, M., & Rejaeian, M. (2014). A comparison between numerical and analytical modeling of ECAP. Iranian Journal of Materials Forming, 1(1), 56-63.

[21] Perig, A. V. (2014). 2D upper bound analysis of ECAE through 2θ-dies for a range of channel angles. Materials Research, 17, 1226-1237.

[22] Vaseghi, M. (2015). Modeling of deformation behavior and dynamic strain ageing in ECAP. Procedia Materials Science, 11, 418-422.

[23] Djavanroodi, F., Omranpour, B., Ebrahimi, M., & Sedighi, M. (2012). Designing of ECAP parameters based on strain distribution uniformity. Progress in natural science: Materials international, 22(5), 452-460.

[24] Djavanroodi, F., & Ebrahimi, M. (2010). Effect of die parameters and material properties in ECAP with parallel channels. Materials Science and Engineering: A, 527(29-30), 7593-7599.

[25] Aghaie-khafri, M., & Rejaeian, M. (2014). A comparison between numerical and analytical modeling of ECAP. Iranian Journal of Materials Forming, 1(1), 56-63.

[26] Patil, B. V., Chakkingal, U., & Kumar, T. P. (2015). Effect of geometric parameters on strain, strain inhomogeneity and peak pressure in equal channel angular pressing–A study based on 3D finite element analysis. Journal of Manufacturing Processes, 17, 88-97.

[27] Park, J. W., & Suh, J. Y. (2001). Effect of die shape on the deformation behavior in equal-channel angular pressing. Metallurgical and materials transactions A, 32(12), 3007-3014.

[28] Ding, R., Chung, C., Chiu, Y., & Lyon, P. (2010). Effect of ECAP on microstructure and mechanical properties of ZE41 magnesium alloy. Materials Science and Engineering: A, 527(16-17), 3777-3784.

[29] Kočiško, R., Kvačkaj, T., & Kováčová, A. (2014). The influence of ECAP geometry on the effective strain distribution. Journal of Achievements in Materials and Manufacturing Engineering, 62(1), 25-30.

[30] Han, J. H., Chang, H. J., Jee, K. K., & Oh, K. H. (2009). Effects of die geometry on variation of the deformation rate in equal channel angular pressing. Metals and Materials International, 15(3), 439-445.

[31] Naik, G. M., Bandadka, S., Mallaiah, M., Badiger, R. I., & Sannayellappa, N. (2020). Effect of ECAE Die Angle on Microstructure Mechanical Properties and Corrosion Behavior of AZ80/91 Magnesium Alloys. Magnesium Alloys Structure and Properties, 3.

[32] Naik, G. M., Narendranath, S., & Kumar, S. S. (2019). Effect of ECAP die angles on microstructure mechanical properties and corrosion behavior of

AZ80 Mg alloy. Journal of Materials Engineering and Performance, 28(5), 2610-2619.

[33] Furuno, K., Akamatsu, H., Oh-Ishi, K., Furukawa, M., Horita, Z., & Langdon, T. G. (2004). Microstructural development in equal-channel angular pressing using a 60 die. Acta Materialia, 52(9), 2497-2507.